Applied Physics A (2024) 130:103
https://doi.org/10.1007/s00339-024-07284-2

Applied Physics A
Materials Science & Processing

A study on the dark and illuminated operation of Al/Si_3N_4/p-Si Schottky photodiodes: optoelectronic insights

Ozge Surucu[1] · Dilber Esra Yıldız[2] · Murat Yıldırım[1,2,3]

Received: 3 November 2023 / Accepted: 2 January 2024
© The Author(s) 2024

Abstract

This work extensively investigates the operation of an Al/ Si_3N_4/p-Si Schottky-type photodiode under dark and varying illumination intensities. The photodiode is fabricated by employing the metal–organic chemical vapor deposition (MOCVD) method. A thorough electrical characterization is performed at room temperature, encompassing measurements of current–voltage (*I*–*V*), current–time (*I*–*t*), capacitance–time (*C*–*t*), and conductance time (*G*–*t*). The photodiode's rectification factor and reverse bias area increased under illumination. The relationship between light power density, barrier height, and diode ideality factor is found. The study also found a strong correlation between light intensity and applied voltage on series resistance (R_s) and shunt resistance (R_{sh}). R_s values are calculated using Cheung's functions, revealing the diode's resistance behavior. The study also examines the photodiode's photoconductivity and photoconductance, finding a non-linear relationship between photocurrent and illumination intensity, suggesting bimolecular recombination. Calculated photosensitivity (*K*), responsivity (*R*), and detectivity (*D**) values show the device's light response effectiveness, but efficiency decreases at higher illumination intensities. Transient experiments indicate stable and reproducible photocurrent characteristics, revealing photogenerated charge temporal evolution. This study provides a complete understanding of the Al/Si_3N_4/p-Si Schottky photodiode's behavior under different illumination intensities. The findings advance optoelectronic device knowledge and enable their use in advanced technologies.

Keywords Photodiode · Schottky diode · Electrical characterization · Si_3N_4 · Si · MIS

1 Introduction

Silicon (Si) has long been employed as a fundamental constituent in electronic devices due to its exceptional properties as a semiconductor. However, owing to its inherent limitations in terms of direct bandgap and suboptimal light emission properties, it has conventionally been regarded as less appropriate for optoelectronic applications [1–4]. The resolution of these obstacles requires the development of creative solutions, prompting researchers to investigate heterojunction structures in silicon-based devices. Significant advancements have been achieved through the integration of dielectric layers such as Si_3N_4, SiC, or SiO_2 [3, 4]. The addition of these layers has not only improved the optical and electrical characteristics but has also expanded the range of wavelengths that can be absorbed to include the ultraviolet (UV) spectrum. This development has created new possibilities for the advancement of optoelectronic devices [1, 2].

SiC, Si_3N_4, and SiO_2 have emerged as significant choices within the domain of dielectric matrices. Silicon dioxide (SiO_2), due to its larger bandgap in comparison to silicon nitride (Si_3N_4), produces elevated barriers that have a substantial impact on the transport properties [3–5]. The Si_3N_4/Si interface has attracted significant interest in the scientific community because of its enhanced carrier tunneling probability and reduced barrier height, rendering it a highly promising option for Si-based devices. It has been observed by researchers that the conductance of Si_3N_4/Si interfaces is higher compared to SiO_2/Si interfaces. This difference in conductance is attributed to an increased probability of tunneling [5, 6]. In addition, the utilization of Si_3N_4 passivation

✉ Dilber Esra Yıldız
desrayildiz@hitit.edu.tr

[1] Department of Electrical and Electronics Engineering, Atilim University, 06836 Ankara, Turkey

[2] Department of Physics, Faculty of Arts and Sciences, Hitit University, 19030 Corum, Turkey

[3] Department of Biotechnology, Faculty of Science, Selcuk University, 42130 Konya, Turkey

Published online: 16 January 2024

has demonstrated its efficacy in mitigating leakage current, thereby improving the dependability of Si_3N_4/GaN photodiodes. This highlights the diverse range of applications for these dielectric matrices [6–9].

The utilization of photodiodes, particularly the metal–insulator–semiconductor (MIS) configurations, has brought about a significant transformation in the field of light detection technology. The aforementioned devices, which consist of a metal electrode, an insulator layer, and a semiconductor substrate, present a multitude of benefits in comparison to traditional p–n junction photodiodes. The MIS structure is characterized by its ability to minimize dark current, enhance responsivity, and exhibit a selective wavelength spectrum response. These features make it highly valuable in various applications, such as solar-blind UV photodetection and near-infrared sensing, as supported by multiple studies [10–17].

The enhancement of MIS photodiode performance necessitates careful consideration of multiple factors. The crucial factors that significantly impact the performance are the quality of the insulator layer, the density of interface states, the barrier height, and the bandgap of the semiconductor. Various strategies have been investigated by researchers in order to improve the efficiency of MIS photodiodes. An example of an effective approach to enhancing efficiency and reducing noise in AlGaN-based MIS photodiodes within the solar-blind region is the incorporation of a thin n-AlGaN layer with an Al content gradient and a uniform n-AlGaN interlayer [10]. Similarly, AuPd/SiO_2/n-Si metal–insulator–semiconductor (MIS) photodiodes have demonstrated improved photosensitivity and restricted bandwidth in the near-infrared range. The aforementioned accomplishment is a consequence of integrating a transparent electrode composed of AuPd, along with the reduction of interface state density through surface chemical treatment and rapid thermal oxidation [11]. Furthermore, the utilization of a tunnel-transparent oxide layer in InAs-based MIS photodiodes has been successful in achieving high speed and low capacitance, effectively reducing tunneling resistance [17].

This paper examines the complexities of Al/Si_3N_4/p-Si Schottky-type photodiode, with a focus on their novel heterojunction structures and dielectric layers, in order to contribute to the progress of optoelectronic devices. Through a comprehensive analysis of these innovative methodologies, the main aim of the present work is to make a valuable contribution to the continuous advancement of optoelectronics. This endeavor involves tackling the obstacles presented by the inherent limitations of silicon and driving the field toward unexplored frontiers.

2 Experimental details

A p-type Si wafer, which has 7.3×10^{15} cm^{-3} carrier concentrations, one-side polished, and (100) orientation, is employed for obtaining the Al/Si_3N_4/p-Si Schottky-type photodiode. The wafer pieces (around 1×2 cm^2) are cleaned in an ultrasonic bath with isopropanol, acetone, and deionized water solvents. The pieces are submerged in the HF:H_2O (1:10) solution for only 30 s to remove the undesired oxide layer. To form an ohmic back contact, Al metals are deposited on the unpolished side of the wafers as 150 nm thick. After deposition, the wafers are annealed at 400 °C under a N_2 atmosphere for 3 min. Then, a metal–organic chemical vapor deposition (MOCVD) system is used to deposit the Si_3N_4 layer on the bare (polished) surface of the p-Si/Al substrate. During the deposition, the substrate temperature is kept at 200 °C, and a 5 nm thick Si_3N_4 film layer is deposited with ammonia (NH_3) and disilane (Si_2H_6) gas flows. The Al rectifier/Schottky contacts, having 0.00785 cm^2 area with 100 nm thickness, are formed onto the Si_3N_4/p-Si structure using a metal shadow mask in the previously mentioned thermal evaporation system. Finally, the Al/Si_3N_4/p-Si Schottky-type structure shown schematically in Fig. 1 is obtained. The current–voltage (*I*–*V*), current–time (*I*–*t*), capacitance–time (*C*–*t*), and conductance–time (*G*–*t*) characteristics of the Al/Si_3N_4/p-Si Schottky-type photodiodes are obtained with the Fytronix FY-7000 solar simulator measurement system (see Fig. 1) under different power intensities of light illumination.

3 Results and discussion

The energy band diagram and surface scanning electron microscope (SEM) image for the Al/Si_3N_4/p-Si Schottky-type photodiode are shown in Fig. 2. These visual representations provide valuable insights into the structural and electronic properties of the fabricated photodiode, allowing for a more complete understanding of its performance and behavior.

Characterizing a fabricated photodiode electrically holds significant importance. As these devices rely on metal–semiconductor connections that are semiconductor-based, it is imperative to ascertain crucial electrical properties. In this particular context, an analysis is conducted on the current–voltage measurements of the manufactured devices, which are obtained under conditions of room temperature and in a dark environment. Furthermore, the experimental procedure involves conducting current–voltage measurements at varying light intensities to ascertain

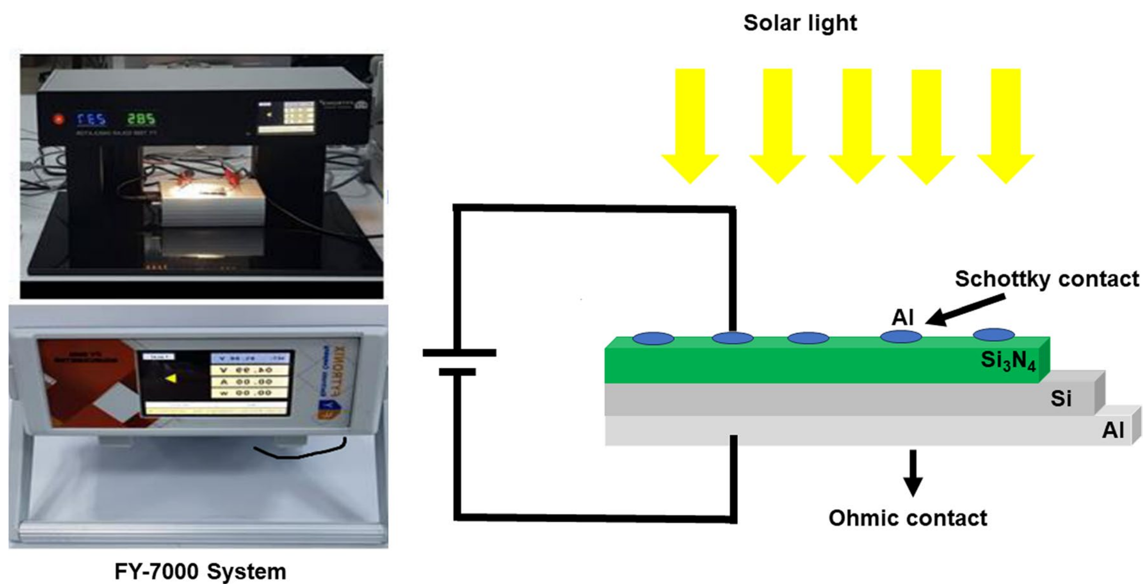

Fig. 1 The Fytronix FY-7000 solar simulator measurement system and schematic diagram of the Al/Si_3N_4/p-Si Schottky-type photodiode

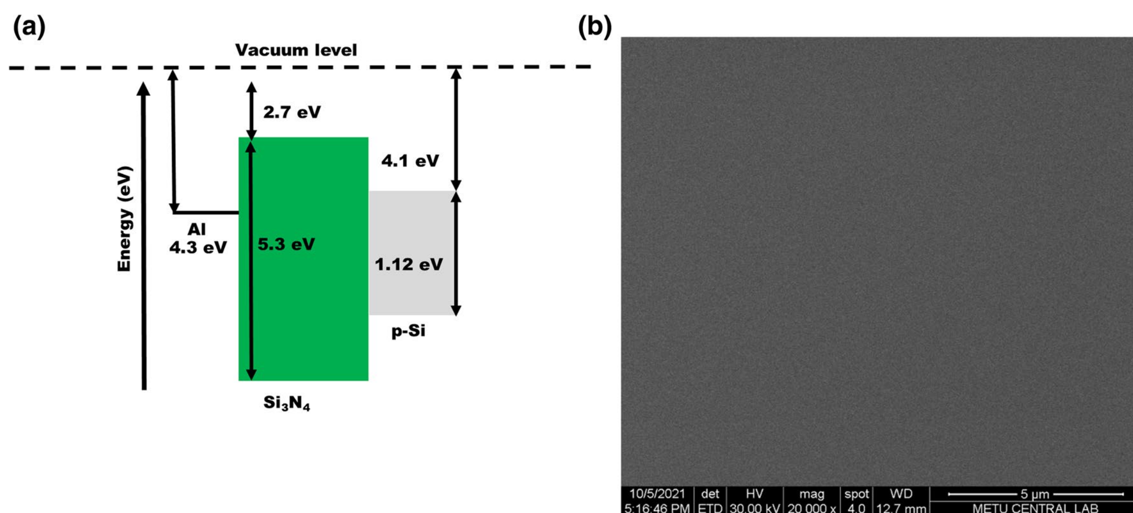

Fig. 2 **a** The schematic and the energy band diagram and **b** surface SEM image for the Al/Si_3N_4/p-Si Schottky-type photodiodes

the light sensitivity of the devices. The resulting characteristics are presented in Fig. 3. As seen in the figure, the photodiode composed of Al/Si_3N_4/p-Si demonstrates a significant improvement in its rectification factor and an appreciable expansion in the reverse bias area when subjected to illumination. This phenomenon can be elucidated by the thermionic emission model. When exposed to light, the photogenerated carriers within the silicon (Si) substrate become energized and transition to higher energy states, facilitating thermionic emission across the interface between the metal and semiconductor. This event leads to a substantial increase in the rectification factor, which signifies enhanced efficiency of the diode (see Fig. 3a). In addition, the observed rise in the reverse bias area might be ascribed to the heightened efficiency of carrier generation and collection resulting from illumination. The behavior under consideration can be explained by the thermionic emission model (TE), which suggests that the presence of illumination enables the carriers to overcome the potential barrier and leave, resulting in a significant increase in the reverse bias area [18–20]. The aforementioned behavior highlights the significant influence of illumination on the electrical properties of the Al/Si_3N_4/p-Si photodiode, providing insights into its possible utilization in sophisticated optoelectronic devices.

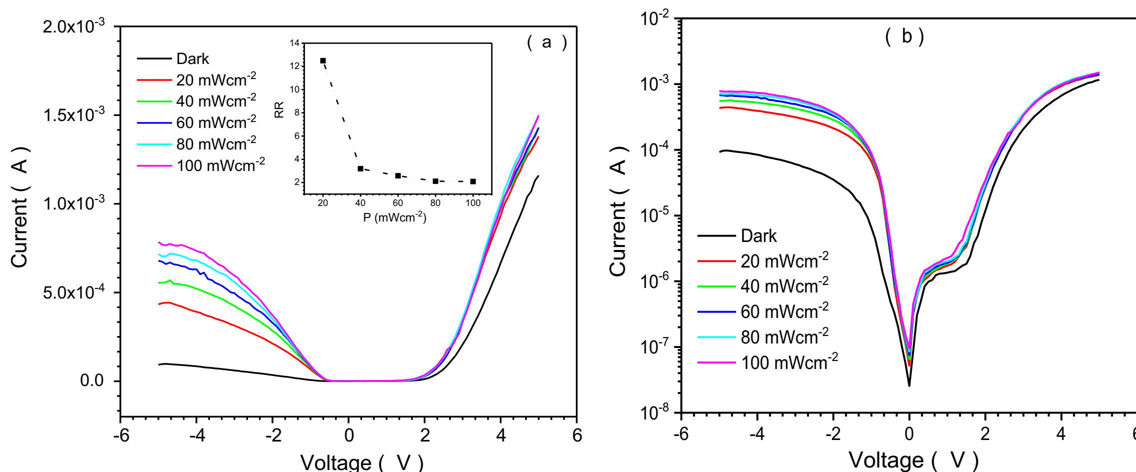

Fig. 3 The linear (**a**) and the semilogarithmic (**b**) *I–V* characteristics of the Al/Si_3N_4/p-Si photodiode (The rectification factor (RR) vs. illumination intensity (P) plot is given as implemented in Fig. 4a)

The TE model states that the net current, considering the voltage drop caused by the presence of series resistance (R_s), can be mathematically represented as [19]

$$I = I_0\left[\exp\left(\frac{q\left(V - IR_s\right)}{nkT}\right) - 1\right]. \quad (1)$$

In the given equation, the symbol "n" represents the ideality factor, "V" denotes the applied voltage, "q" represents the electronic charge, "T" signifies the temperature measured in Kelvin, and k denotes the Boltzmann constant. Furthermore, the coefficient "I_0" represents the saturation current and is associated with the barrier height ($\varnothing_B$) of the diode due to the following relationship:

$$I_0 = AA^*\left[\exp\left(-\frac{q}{kT}\right)\varnothing_B\right]. \quad (2)$$

The variables "A" and "A^*" represent diode area and the Richardson constant, respectively. The Richardson constant for p-Si is 32 A/K^2.cm^2, and the diode area is 0.00785 cm^2.

The evaluation of a photodiode's performance involves the assessment of two significant parameters: barrier height and diode ideality factor. The barrier height and diode ideality factors exhibit variability and are dependent on multiple factors, including temperature, doping concentration, interface states, and illumination intensity. The power density of the light that hits the diode can change the carrier concentration and recombination rate in the depletion zone of the junction, which can change the barrier height and ideality factor.

Figure 4a illustrates a relationship between the power density of light and two parameters: the barrier height and the diode ideality factor. It is observed that as the power density of light increases, the barrier height drops while the diode ideality factor increases. This phenomenon may be elucidated because the carriers induced by light have the effect of diminishing the effective height of the barrier by reducing the width of the Schottky barrier depletion and simultaneously augmenting the current of recombination by intensifying the processes of generation and recombination in the region of charge inside the space. These effects lead to a departure from the ideal current–voltage (*I–V*) characteristics and an elevation in the diode ideality factor [21–24]

In order to enhance the performance of a diode, it is imperative to maintain a minimal level of series resistance. The resistance observed in the diode can be attributed to two main factors: the inherent characteristics of the diode's structure and contact areas, and the influence of interface states present in the junction. Conversely, higher shunt resistance (R_{sh}) values are associated with a rise in leakage currents. The behavior of these currents can be influenced by the presence of contacts and surface inhomogeneities, which can impact the current components through the presence of localized states and the formation of an accumulation layer at the surface [25].

The parasitic resistance, given as R_i, for the Al/Si_3N_4/p-Si photodiode is determined using the equation $R_i = \partial V/\partial I$. A variation in the value of R_i is detected with changes in illumination, as depicted in Fig. 4b across the whole range of the bias voltage spectrum. The research demonstrates a negative correlation between resistance values and voltage, indicating that resistance decreases as voltage increases. In addition, the analysis reveals a significant relationship between resistance values and illumination, suggesting a high dependence on the level of light. The observed phenomenon of resistance increasing with increasing light can be attributed to the higher number of bonds breaking or de-trapping of charge carriers on both sides of the bias regions because of increased illumination [18,

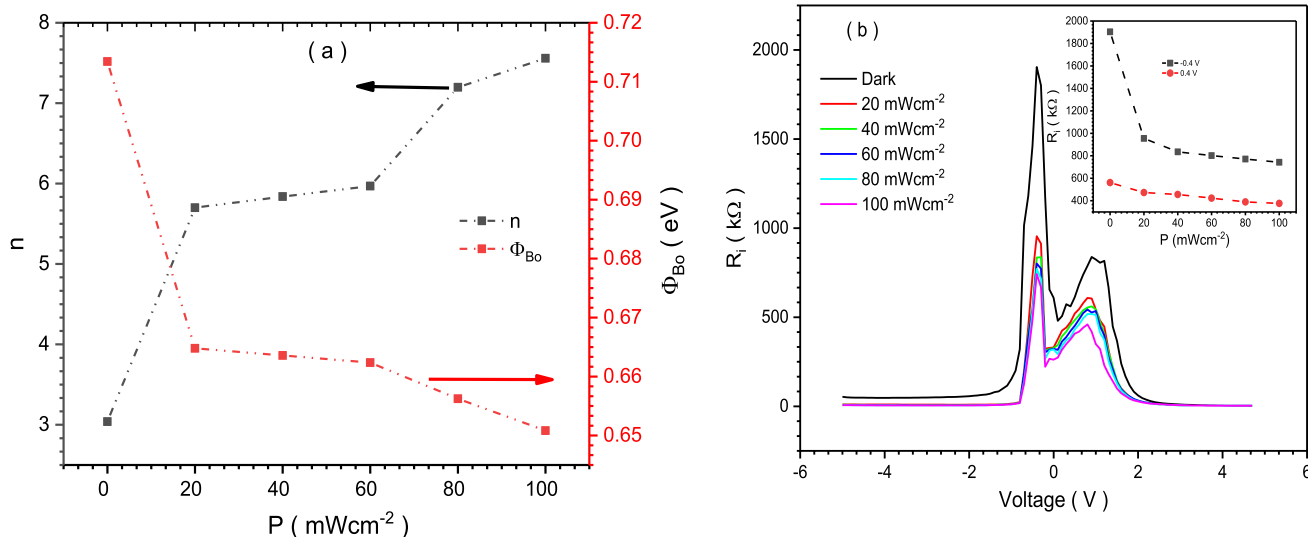

Fig. 4 The trends for n and $\varnothing_B$ with the illumination intensity (P) (**a**), Ri vs. V plot under dark and varying illuminations for the Al/Si_3N_4/p-Si photodiode. (The trend for R_i with varying illumination intensities at – 0.4 and 0.4 V is given as implemented in (**b**)

Table 1 Calculated some electrical parameters for Al/Si_3N_4/p-Si photodiode

P (mW/cm^2)	n	$\varnothing_{B0}$(eV)	I_o (A)	R_s (W)	
				dV/d$LN(I)$	$H(I)$
0	3.039	0.713	2.40×10^{-8}	2183	2152
20	5.700	0.665	1.57×10^{-7}	2069	1588
40	5.838	0.664	1.65×10^{-7}	1994	1537
60	5.970	0.662	1.72×10^{-7}	1787	1524
80	7.197	0.656	2.19×10^{-7}	1732	1422
100	7.559	0.651	2.69×10^{-7}	1709	1404

26]. The figures presented in Fig. 4a, b indicate that both the values of R_{sh} and R_s exhibit considerable sensitivity to both light intensity and applied voltage. Figure 4b indicates the relationship between resistance value and light intensity, represented as a function of voltage. This observation suggests that the resistance of the photodiode can be affected by both the intensity of the incident light and the applied voltage (see Table 1).

Cheung's functions can be used to figure out the series resistance R_s values for Al/Si_3N_4/p-Si photodiode when the illumination intensity changes. This method is widely used in the analysis of a diode. In addition, the Cheung functions are given in the following equations [27]:

$$\frac{dV}{d(\ln I)} = \left(\frac{nkT}{q}\right) + IR_s \tag{3}$$

$$H(I) = V - n\frac{kT}{q}\ln\left(\frac{I}{AA^*T^2}\right) = n\varnothing_B + IR_s. \tag{4}$$

The $dV/d\ln(I)$ versus I and the $H(I)$ versus I plots are given in Fig. 5a, b, respectively.

Previously, the Al/Si_3N_4/p-Si photodiode is discussed in detail by examining its characteristics using the thermionic emission model as a framework. By means of precise examination, the critical parameters are examined, including resistivity, barrier height, and diode ideality factors, thereby revealing the key components that govern its operation.

In order to further validate the results and offer a comprehensive analysis, we shall now shift our focus to the domains of photoconductivity and photoconductance. With the aim of clarifying the manner in which the photodiode reacts to incident light, the exact measurements of photoconductivity are carried out. By determining the photosensitivity, responsivity, and other important features of the device, this undertaking seeks to provide significant knowledge regarding its optoelectronic characteristics. By investigating photoconductivity and associated phenomena, we aim to uncover previously undiscovered realms of comprehension, thereby facilitating the development of improved photodetector technologies and applications.

The photoconductivity mechanism of the Al/Si_3N_4/p-Si photodiode is analyzed by the following relation [18, 28]:

$$I_{ph} = AP^m, \tag{5}$$

where A, P, and m are the proportionality constant, illumination intensity, and exponent of the relation, respectively.

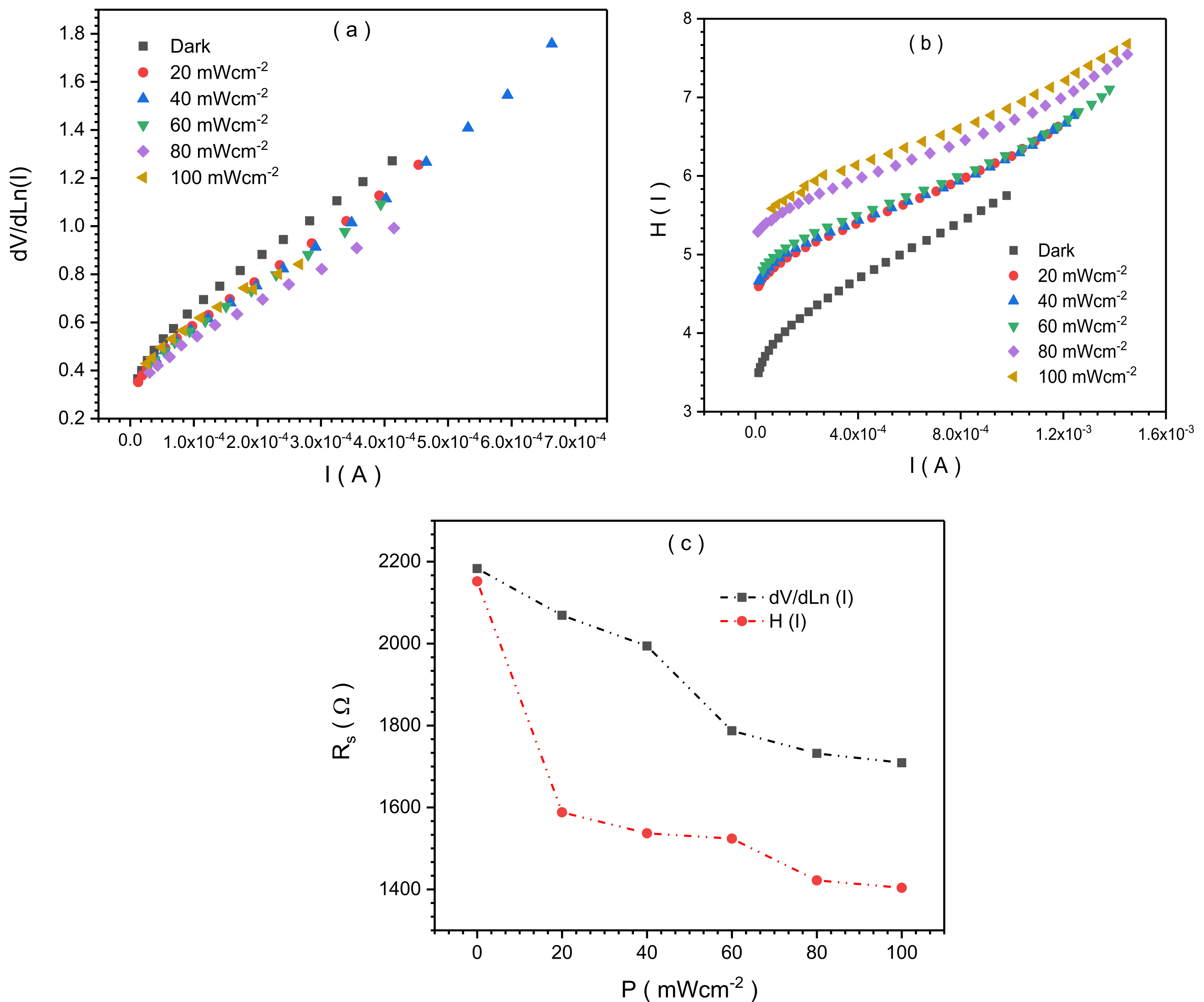

Fig. 5 **a** The d*V*/dLn*(I)* vs. *I* characteristics, **b** *H(I)* vs *I* plot, and **c** *Rs* vs *P* plots for Al/Si_3N_4/p-Si photodiode

As denoted by the exponent *m*, the relationship between photocurrent and illumination intensity is established. When *m* equals 0.5, the relationship between photocurrent and illumination intensity becomes non-linear, suggesting that charge carriers engage in a bimolecular recombination mechanism. On the contrary, when *m* approaches unity, a linear relationship is observed between photocurrent and light intensity. This finding implies that charge carriers operate according to the principle of monomolecular recombination [29]. In order to determine the exponent *m* for the Al/Si_3N_4/p-Si photodiode, the log(I_{ph}) versus log(P) graph is plotted as seen in Fig. 6a, and it is found as 0.44, indicating the bimolecular recombination mechanism.

Photosensitivity (K), an essential criterion for evaluating the performance of photodetectors, is a fundamental attribute that defines the capacity of a photodiode to transform incident light into an electrical signal. K, which is frequently calculated as the ratio of photocurrent (I_{ph}) to dark current (I_d), provides a key indicator of a photodetector's effectiveness in responding to light. Higher photosensitivity values denote a greater ability to harness and amplify the impact of incident photons, underlining the device's aptitude for light detection [29]. The obtained photosensitivity (K) values for Al/Si_3N_4/p-Si photodiode with varying illumination intensities are given in Table 2, and their trend is shown in Fig. 6b. As expected, with the increasing illumination intensity, K values are increasing.

An additional crucial metric for determining the efficiency with which a photodetector converts incoming photons into an electrical response is photoresponsivity (R). It signifies the degree of efficiency at which an apparatus produces a photocurrent in reaction to incident light. A

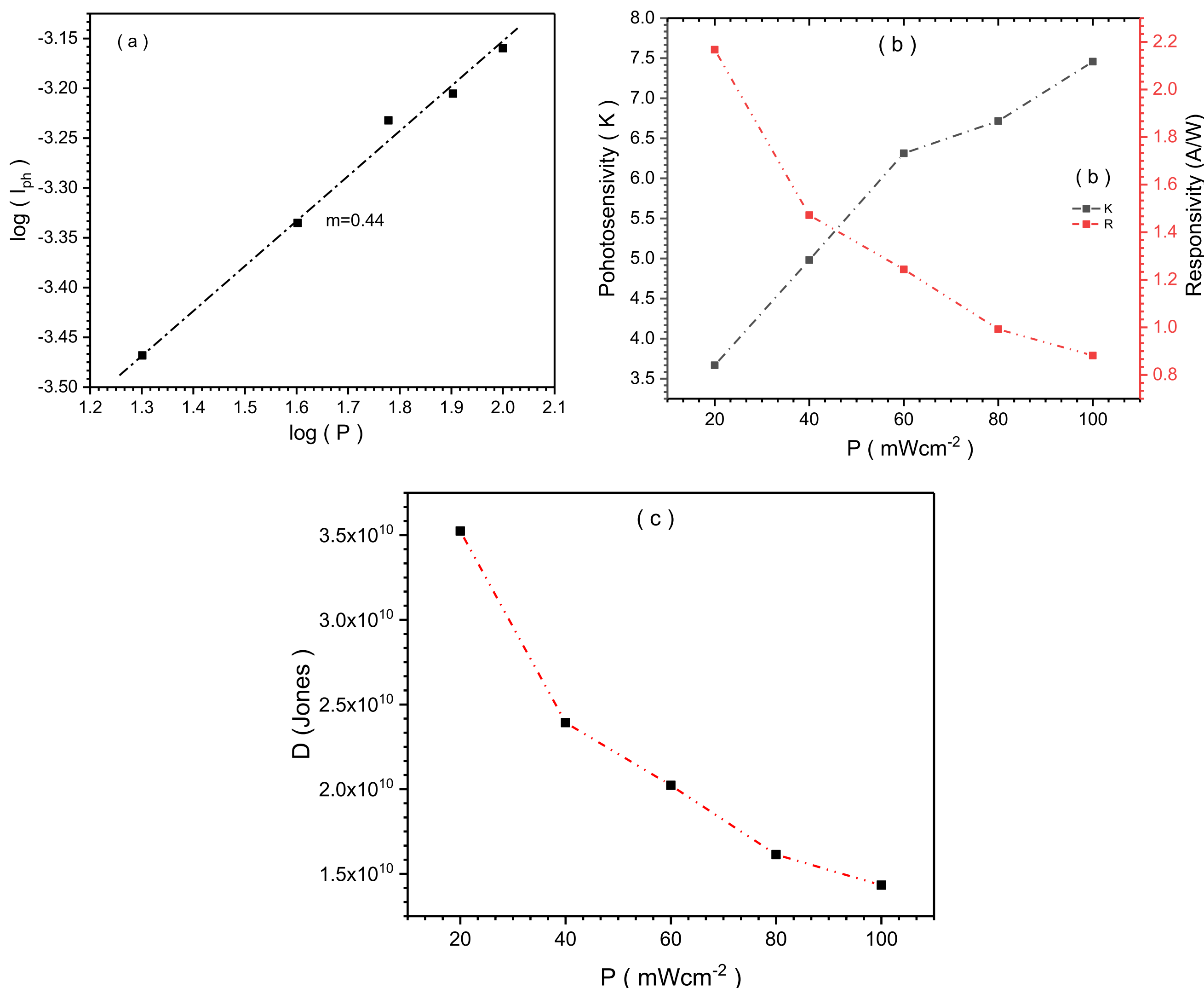

Fig. 6 **a** log(I_{ph}) vs. log(P), **b** K and R vs. P, and **c** D* vs P plots for the Al/Si_3N_4/p-Si photodiode

Table 2 $I_{ph,}$ Photosensitivity (K), responsivity, and detectivity (D*) values for Al/Si_3N_4/p-Si photodiode under varying illumination intensities

P (mW/cm^2)	I_{ph}(μA)	K	Responsivity (m A/W)	Detectivity (D*) (Jones)×10^{10}
20	34.0	3.667	2168	3.52
40	46.2	4.980	1472	2.39
60	58.6	6.314	1244	2.02
80	62.3	6.716	992	1.61
100	69.2	7.457	882	1.43

photodiode with a high photoresponsivity value demonstrates remarkable capability in capturing and transforming light into an electrical signal that can be detected. The responsivity is defined by the ratio of photocurrent density to the illumination intensity, which can be determined as follows [18, 29]:

$$R = \frac{I_{ph} - I_d}{PA}, \tag{6}$$

where A represents the diode active detector area.

The obtained R values for Al/Si_3N_4/p-Si photodiode with varying illumination intensities are given in Table 2, and their trend is shown in Fig. 6b. As can be deduced from the figure, the R values are decreasing with the increasing illumination intensity. The observed phenomenon of a decrease in responsivity with an increase in light intensity is commonly observed in photoconductivity photodetectors. The presence of intense illumination at high power levels leads to a decrease in the number of photogenerated carriers that can be extracted. This reduction

can be attributed to either the Auger process or the saturation of recombination/trap states, both of which have an impact on the lifetime of the generated carriers [30, 31]. When the average responsivity value of 1350 mA/W for the Al/Si_3N_4/p-Si photodiode under different light conditions is compared to values reported in the literature, the findings within this study are notably exceptional. As an illustration, when comparing photodetectors employing Si_3Ni_4 interfaces with Yb-doped V_2O_5 interfaces, the mean responsivity is around 26 mA/W, notwithstanding the variation in Yb doping ratios [32]. Photodetectors utilizing a Ce-doped V_2O_5 interface demonstrate the greatest responsivity at 65.86 mA/W [33], according to a separate study that utilized a La-doped V_2O_5 interface and reported values ranging from 10.33 to 156.21 mA/W [34]. A distinct inquiry was conducted utilizing a Ce–WO_3 interface, wherein the highest achievable responsivity measured 20.61 mA/W [35]. Based on its average responsivity of 1350 mA/W, for Al/Si_3N_4/p-Si photodiode photodetector exhibits enhanced performance in comparison to the aforementioned studies, thereby suggesting its capability to detect light with high efficiency.

In addition, detectivity (D^*), when combined with photoresponsivity, is an essential parameter for assessing the performance of a photodetector under low-light conditions. The metric of detectivity represents the ability of a photodiode to differentiate weak signals from a background of noise. This is crucial for applications that require high sensitivity, even in low-light conditions [18, 29]. The values D^* for Al/Si_3N_4/p-Si photodiode are obtained using the following relation, and their values with varying illumination intensities are given in Table 2, and their trend is shown in Fig. 6c [18]:

$$D^* = R\sqrt{\frac{A}{2qI_d}}, \tag{7}$$

where q represents the elementary charge ($q = 1.6 \times 10^{-19}$ C.).

The parameters R and D^* exhibit a decrease as the illumination intensity increased. Therefore, it is advisable to consider an optimal load line for the photodiode to achieve optimal sensitivity, responsivity, and detectivity. Moreover, the Al/Si_3N_4/p-Si photodiode has achieved a remarkable detectivity (D*) value, reaching an impressive 3.52×10^{10} Jones. The device's exceptional detectivity highlights its effectiveness in detecting low levels of light intensity. In order to provide context for the findings, the results are compared to those reported in the existing literature on other material interfaces. As an example, the Yb-doped V_2O_5 interface has been reported to have a detectivity of 9.97×10^{10} Jones [32], demonstrating the strong performance of the Al/Si_3N_4/p-Si photodiode in comparison to others. In studies examining La-doped V_2O_5 interfaces, the highest detectivity achieved is 9.82×10^{10} Jones [34], whereas for Ce-doped V_2O_5 interfaces, the maximum reported value is 2.99×10^{10} Jones [33]. The detectivity of the Al/Si_3N_4/p-Si photodiode, although slightly lower than the peak values in these specific cases, remains within a commendable range, affirming its effectiveness for applications requiring superior sensitivity to low-light levels.

The transient experiments conducted on the Al/Si_3N_4/p-Si photodiode yield significant insights regarding the temporal evolution of photogenerated charges and their

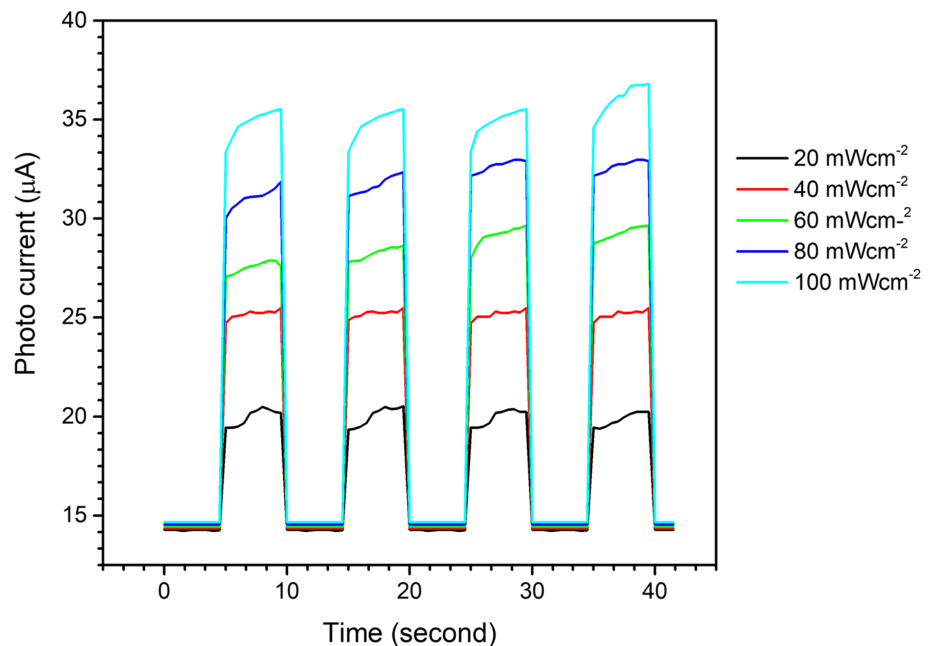

Fig. 7 Transient photocurrent measurements for Al/Si_3N_4/p-Si photodiode

density. Figure 7 illustrates the relationship between current and time during alternating periods of darkness and varying illumination, utilizing an ON/OFF shift lasting 10 s in duration. Under the presence of illumination, the photocurrent exhibits a notable increase until reaching a steady state. Subsequently, upon an absence of illumination, the photocurrent experiences a significant decrease, ultimately returning to its initial value. This behavior demonstrates remarkable stability and reproducibility in the characteristics of the photocurrent [18, 30, 31].

Figure 8a, b illustrates the transient photocapacitance and photoconductance characteristics of a photodiode under various illumination intensities at the frequency of 10 Hz, respectively.

Figure 8 indicates that the photocapacitance experiences an abrupt surge when the illumination power is activated, followed by a swift decline to its initial value when the power is deactivated. The observed behavior may be attributed to the fluctuation in carrier density produced by photons during the transition from the on or off states. The behavior of the photoconductance is comparable between the on and off states [23, 36].

4 Conclusion

This study intends to comprehensively investigate the behavior of the Al/Si_3N_4/p-Si Schottky-type photodiode across a variety of illumination intensities. The Al/Si_3N_4/p-Si

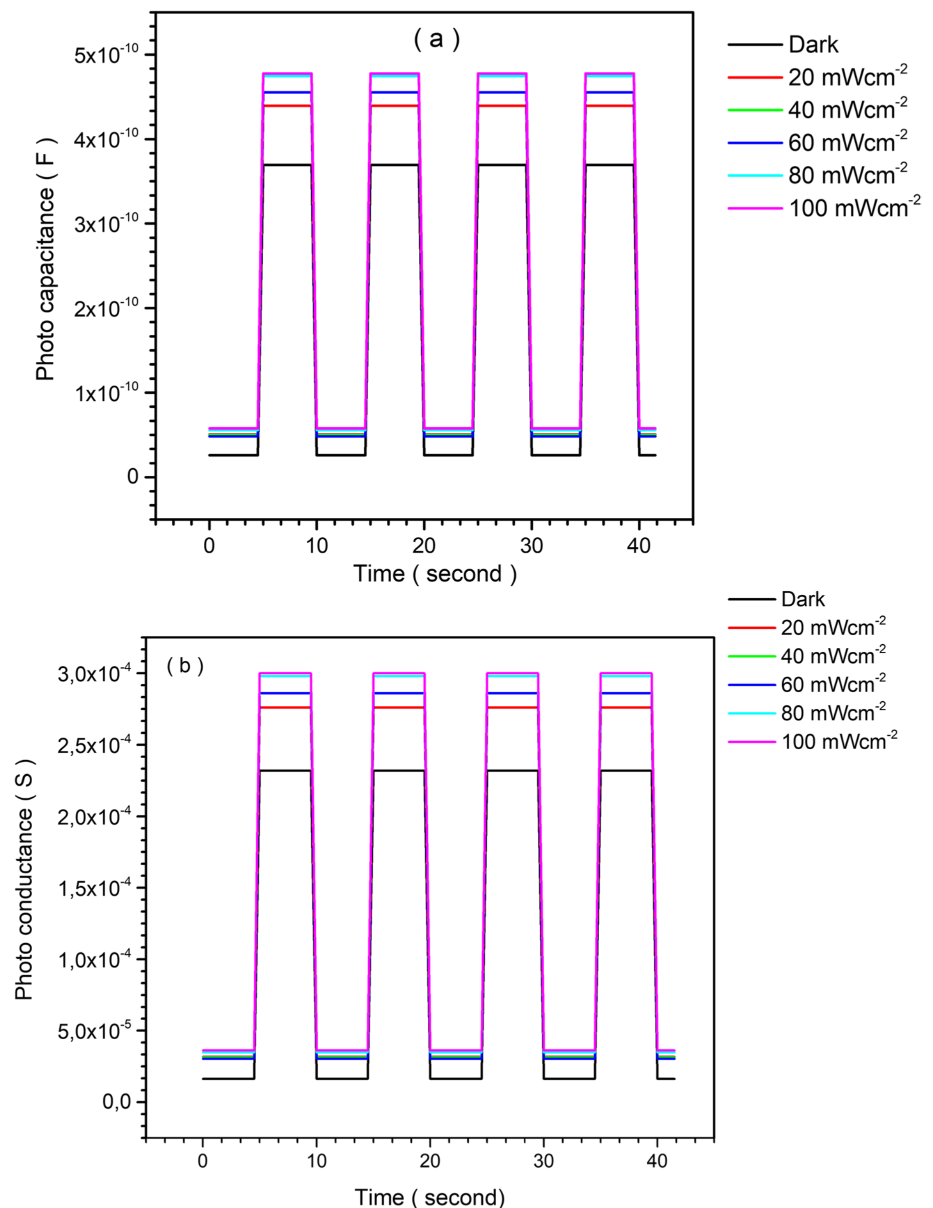

Fig. 8 Transient **a** photocapacitance and **b** photoconductance characteristics for Al/Si_3N_4/p-Si photodiode

photodiode displays interesting characteristics upon exposure to light. The experiment reveals a substantial increase in the rectification factor and a significant widening of the reverse bias region under the effect of illumination. The thermionic emission model is employed to explain this phenomenon, wherein the photogenerated carriers within the silicon substrate underwent transitions to higher energy states, facilitating thermionic emission across the interface between the metal and semiconductor.

It is observed that as the intensity of the illumination increases, the diode ideality factor (n) increases from 3.039 in the dark to 7.559 under 100 mW/cm^2 illumination. In contrast, under 100 mW/cm^2 illumination, the barrier height ($\varnothing_{B0}$) decreases from 0.713 eV in the dark to 0.651 eV. Light-induced carriers are responsible for these changes in critical parameters, which reduce the effective barrier height by narrowing the Schottky barrier depletion width and intensifying recombination processes, resulting in deviations from ideal diode characteristics.

Furthermore, the study emphasizes the relationship between illumination levels and series resistance. The parasitic resistance (R_i) study discovered an inverse relationship between resistance and voltage, implying that resistance decreases as voltage increases. Furthermore, a significant correlation between resistance values and illumination highlights the impact of light intensity on diode resistance. Further investigations utilizing Cheung's functions yields significant results regarding the changes in series resistance (R_s) in relation to different levels of illumination intensity. The study of photoconductivity reveals the presence of a bimolecular recombination mechanism. The obtained photosensitivity (K) values, which are determined as 3.667 in the dark and 7.457 under the illumination of 100 mW/cm^2, demonstrate a positive relationship with light intensity. This suggests that the device exhibits a high level of effectiveness in detecting light. On the contrary, there is a decrease in the responsivity (R) values from 2.168 A/W in the dark to 0.882 A/W when exposed to the illumination of 100 mW/cm^2. In the same manner, the values of detectivity (D^*) exhibit a decrease from 3.52 Jones in the dark to 1.43 Jones when subjected to an illumination intensity of 100 mW/cm^2. As the intensity of illumination increases, there is a parallel decrease in both the R and D* values. This highlights the importance of optimizing the load line of the photodiode in order to achieve maximum sensitivity, responsivity, and detectivity.

Furthermore, the Al/Si_3N_4/p-Si photodiode exhibits consistent patterns during transient experiments: under illumination, the photocurrent increases continuously and subsequently decreases when the light is removed, demonstrating its stable nature. The rapid return of photocapacitance to its initial value following activation and deactivation can be attributed to fluctuations in carrier density induced by photons. Significantly, the photoconductance characteristics show constancy in both the on and off states, signifying an exceptional degree of performance stability for the device.

In conclusion, this extensive investigation not only provides a deeper understanding of the complex behavior exhibited by the Al/Si3N4/p-Si Schottky-type photodiode when subjected to different levels of illumination but also emphasizes its capacity to contribute to the progress of optoelectronic technologies. The study offers valuable insights that can serve as a guiding framework for the advancement of photodetectors with enhanced efficiency and stability, thereby enabling their application in diverse fields.

Acknowledgements The authors gratefully acknowledge the Hitit University of BAP due to the financial support for the Project FEF19004.15.010, FEF19002.15.001, and FEF01.13.003.

Author contributions OS: writing—review and editing, writing—original draft, methodology, investigation, conceptualization. DEY: writing—review and editing, writing—original draft, methodology, investigation, conceptualization, supervision. MY: writing—review and editing, methodology, investigation.

Funding Open access funding provided by the Scientific and Technological Research Council of Türkiye (TÜBİTAK).

Data availability Data will be made available on request.

Declarations

Conflict of interest The authors declare that they have no known competing financial interests or personal relationships that could have appeared to influence the work reported in this paper.

Open Access This article is licensed under a Creative Commons Attribution 4.0 International License, which permits use, sharing, adaptation, distribution and reproduction in any medium or format, as long as you give appropriate credit to the original author(s) and the source, provide a link to the Creative Commons licence, and indicate if changes were made. The images or other third party material in this article are included in the article's Creative Commons licence, unless indicated otherwise in a credit line to the material. If material is not included in the article's Creative Commons licence and your intended use is not permitted by statutory regulation or exceeds the permitted use, you will need to obtain permission directly from the copyright holder. To view a copy of this licence, visit http://creativecommons.org/licenses/by/4.0/.

References

1. A.K. Panchal, C.S. Solanki, Fabrication of silicon quantum dots in SiNx multilayer using hot-wire CVD. J. Cryst. GrowthCryst. Growth **311**, 2659–2663 (2009). https://doi.org/10.1016/j.jcrysgro.2009.03.013
2. F. Gourbilleau, C. Dufour, B. Rezgui, G. Brémond, Silicon nanostructures for solar cell applications. Mater. Sci. Eng. B Sci. Eng. B **159–160**, 70–73 (2009). https://doi.org/10.1016/j.mseb.2008.10.052
3. G. Conibeer, M. Green, R. Corkish, Y. Cho, E.-C. Cho, C.-W. Jiang, T. Fangsuwannarak, E. Pink, Y. Huang, T. Puzzer, T. Trupke, B. Richards, A. Shalav, K. Lin, Silicon nanostructures

for third generation photovoltaic solar cells. Thin Solid Films **511–512**, 654–662 (2006). https://doi.org/10.1016/j.tsf.2005.12.119
4. F. Sohrabi, A. Nikniazi, H. Movl, Optimization of Third Generation Nanostructured Silicon- Based Solar Cells, in: Solar Cells - Research and Application Perspectives, InTech, (2013). https://doi.org/10.5772/51616.
5. P. Lorenzo, T. Rasit, S. Nanocrystals, Wiley (2010). https://doi.org/10.1002/9783527629954
6. I. Guler, Optical and structural characterization of silicon nitride thin films deposited by PECVD. Mater. Sci. Eng. B **246**, 21–26 (2019). https://doi.org/10.1016/j.mseb.2019.05.024
7. H.L. Hao, L.K. Wu, W.Z. Shen, Controlling the red luminescence from silicon quantum dots in hydrogenated amorphous silicon nitride films. Appl. Phys. Lett. (2008). https://doi.org/10.1063/1.2902296
8. M. Wang, D. Li, Z. Yuan, D. Yang, D. Que, Photoluminescence of Si-rich silicon nitride: Defect-related states and silicon nanoclusters. Appl. Phys. Lett. (2007). https://doi.org/10.1063/1.2717014
9. Y.Q. Wang, Y.G. Wang, L. Cao, Z.X. Cao, High-efficiency visible photoluminescence from amorphous silicon nanoparticles embedded in silicon nitride. Appl. Phys. Lett. **83**, 3474–3476 (2003). https://doi.org/10.1063/1.1621462
10. Q. Cai, H. You, H. Guo, J. Wang, B. Liu, Z. Xie, D. Chen, H. Lu, Y. Zheng, R. Zhang, Progress on AlGaN-based solar-blind ultraviolet photodetectors and focal plane arrays. Light Sci Appl. **10**, 94 (2021). https://doi.org/10.1038/s41377-021-00527-4
11 I.O. Althobaiti, M. Aouassa, S.A. Algarni, A.M. Al Mutairi, A.H. Ahmed, Highly photosensitive AuPd/SiO2/n-Si MIS structure for near-infrared photo detection and energy harvesting. J. Mater. Sci. Mater. Electron.Electron. **34**, 821 (2023). https://doi.org/10.1007/s10854-023-10233-z
12. H. Pal, S. Singh, C. Guo, W. Guo, O. Badami, T. Pramanik, B. Sarkar, Lateral P-N junction photodiodes using lateral polarity structure GaN films: a theoretical perspective. J. Electron. Mater.Mater. **52**, 2148–2157 (2023). https://doi.org/10.1007/s11664-022-10166-z
13. V.G. Kesler, A.A. Guzev, A.P. Kovchavtsev, A.V. Tsarenko, Z.V. Panova, MIS photodiode with an InAs-based tunnel-transparent oxide layer. Optoelectron. Instrum. Data Process. **50**, 87–95 (2014). https://doi.org/10.3103/S8756699014010117
14. M. Raj, C. Joseph, M. Subramanian, V. Perumalsamy, V. Elayappan, Superior photoresponse MIS Schottky barrier diodes with nanoporous:Sn–WO_3 films for ultraviolet photodetector application. New J. Chem. **44**, 7708–7718 (2020). https://doi.org/10.1039/D0NJ00101E
15. D.E. Yıldız, A. Karabulut, İ Orak, A. Turut, Effect of atomic-layer-deposited HfO2 thin-film interfacial layer on the electrical properties of Au/Ti/n-GaAs Schottky diode. J. Mater. Sci. Mater. Electron.Electron. **32**, 10209–10223 (2021). https://doi.org/10.1007/s10854-021-05676-1
16. F. Huang, Z. Wang, C. Chu, Q. Liu, Y. Li, Z. Xin, Y. Zhang, Q. Sun, Z.-H. Zhang, MIS-based GaN Schottky barrier diodes: interfacial conditions on the reverse and forward properties. IEEE Trans. Electron Devices **69**, 5522–5529 (2022). https://doi.org/10.1109/TED.2022.3201831
17. T. Zhang, Y. Zhang, J. Zhang, X. Li, Y. Lv, Y. Hao, Current transport mechanism of high-performance novel GaN MIS diode. IEEE Electron Device Lett. **42**, 304–307 (2021). https://doi.org/10.1109/LED.2021.3051690
18. A. Karabulut, D.E. Yıldız, D.A. Köse, M. Yıldırım, Photosensing performances of heterojunctions-based photodiodes with novel complex interlayers. Mater. Sci. Semicond. Process.Semicond. Process. **146**, 106647 (2022). https://doi.org/10.1016/j.mssp.2022.106647
19. D.K. Schroder, Semiconductor material and device characterization. 3rd ed., Wiley-IEEE Press (2015)
20. B.L. Sharma, *Metal-Semiconductor Schottky Barrier Junctions and Their Applications* (Springer Science & Business Media, 2013)
21. D.E. Yıldız, A. Kocyigit, M. Yıldırım, Comparison of Al/TiO2/p-Si and Al/ZnO/p-Si photodetectors. Opt Mater (Amst). **145**, 114371 (2023). https://doi.org/10.1016/j.optmat.2023.114371
22. A. Kocyigit, M. Yıldırım, D.A. Kose, D.E. Yıldız, Synthesize and characterization of Co-complex as interlayer for Schottky type photodiode. Polym. Bull. **79**, 11389–11408 (2022). https://doi.org/10.1007/s00289-021-04021-0
23. H.H. Gullu, D.E. Yıldız, D.A. Kose, M. Yıldırım, Si-based photosensitive diode with novel Zn-doped nicotinate/nicotinamide mixed complex interlayer. Mater. Sci. Semicond. Process.Semicond. Process. **147**, 106750 (2022). https://doi.org/10.1016/j.mssp.2022.106750
24 A. GencerImer, A. Dere, A.G. Al-Sehemi, O. Dayan, Z. Serbetci, A.A. Al-Ghamdi, F. Yakuphanoglu, Photosensing properties of ruthenium(II) complex-based photodiode. Appl. Phys. A **125**, 204 (2019). https://doi.org/10.1007/s00339-019-2504-1
25. P. Chattopadhyay, The effect of shunt resistance on the electrical characteristics of Schottky barrier diodes. J. Phys. D Appl. Phys. **29**, 823–829 (1996). https://doi.org/10.1088/0022-3727/29/3/047
26. E. Coşkun, H.H. Güllü, İ Candan, Ö. Bayraklı, M. Parlak, Ç. Erçelebi, Device behavior of an In/p-Ag(Ga, In)Te2/n-Si/Ag heterojunction diode. Mater. Sci. Semicond. Process.Semicond. Process. **34**, 138–145 (2015). https://doi.org/10.1016/j.mssp.2015.02.043
27. S.K. Cheung, N.W. Cheung, Extraction of Schottky diode parameters from forward current-voltage characteristics. Appl. Phys. Lett. **49**, 85–87 (1986). https://doi.org/10.1063/1.97359
28. F. Yakuphanoglu, Transparent metal oxide films based sensors for solar tracking applications. Compos. B Eng. **92**, 151–159 (2016). https://doi.org/10.1016/j.compositesb.2016.02.039
29 H. Alzahrani, K. Sulaiman, F.F. Muhammadsharif, S.M. Abdullah, A.Y. Mahmoud, R.R. Bahabry, S.F. Ab Sani, Effect of illumination intensity on a self-powered UV photodiode based on solution-processed NPD:Alq3 composite system. J. Mater. Sci. Mater. Electron.Electron. **32**, 14801–14812 (2021). https://doi.org/10.1007/s10854-021-06034-x
30. P. Yu, X. Yu, W. Lu, H. Lin, L. Sun, K. Du, F. Liu, W. Fu, Q. Zeng, Z. Shen, C. Jin, Q.J. Wang, Z. Liu, Fast Photoresponse from 1T Tin Diselenide Atomic Layers. Adv. Funct. Mater.Funct. Mater. **26**, 137–145 (2016). https://doi.org/10.1002/adfm.201503789
31. R. Zhuo, S. Zuo, W. Quan, D. Yan, B. Geng, J. Wang, X. Men, Large-size and high performance visible-light photodetectors based on two-dimensional hybrid materials SnS/RGO. RSC Adv. Adv. **8**, 761–766 (2018). https://doi.org/10.1039/C7RA11269F
32. V. Balasubramani, J. Chandrasekaran, V. Manikandan, T.K. Le, R. Marnadu, P. Vivek, Upgraded photosensitivity under the influence of Yb doped on V2O5 thin films as an interfacial layer in MIS type Schottky barrier diode as photodiode application. J. Solid State Chem. **301**, 122289 (2021). https://doi.org/10.1016/j.jssc.2021.122289
33. V. Balasubramani, J. Chandrasekaran, T.D. Nguyen, S. Maruthamuthu, R. Marnadu, P. Vivek, S. Sugarthi, Colossal photosensitive boost in Schottky diode behaviour with Ce-V2O5 interfaced layer of MIS structure. Sens Actuators A Phys. **315**, 112333 (2020). https://doi.org/10.1016/j.sna.2020.112333
34. V. Balasubramani, J. Chandrasekaran, V. Manikandan, T.K. Le, R. Marnadu, P. Vivek, Improved photodetector performance of high-k dielectric material (La) doped V2O5 thin films as an interfacial layer in Schottky barrier diodes. Surf. Interfaces **25**, 101297 (2021). https://doi.org/10.1016/j.surfin.2021.101297
35. R. Marnadu, J. Chandrasekaran, S. Maruthamuthu, V. Balasubramani, P. Vivek, R. Suresh, Ultra-high photoresponse with superiorly sensitive metal-insulator-semiconductor (MIS) structured diodes for UV photodetector application. Appl. Surf. Sci. **480**, 308–322 (2019). https://doi.org/10.1016/j.apsusc.2019.02.214

36 O. Dayan, A. GencerImer, M. Tercan, A. Dere, A.G. Al-Sehemi, A.A. Al-Ghamdi, F. Yakuphanoglu, Dye sensitized solar cell-based optoelectronic device using novel [Ru(L1)(L2)(NCS)2] complex. J. Mol. Struct. **1238**, 130464 (2021). https://doi.org/10.1016/j.molstruc.2021.130464

Publisher's Note Springer Nature remains neutral with regard to jurisdictional claims in published maps and institutional affiliations.